Proceeding Paper

Metal Fused Filament Fabrication of AlSi10Mg Aluminum Alloy [†]

E. Galindo [1], M. Maric [2] , A. Avalos Postigo [3], A. Walker [3], M. Conlon [4], K. Azari [4] and M. Brochu [1,*]

1   REGAL Aluminum Research Center, Department of Mining and Materials Engineering, McGill University, Montreal, QC G1V 0A6, Canada; emilio.galindo@mail.mcgill.ca
2   Department of Chemical Engineering, McGill University, Montreal, QC H3A 0C5, Canada; milan.maric@mcgill.ca
3   AON 3D, Montreal, QC H2N 1P4, Canada; abraham@aon3d.com (A.A.P.); andrew@aon3d.com (A.W.)
4   Equispheres Inc., Ottawa, ON K2V 1C2, Canada; martin.conlon@equispheres.com (M.C.); kamran.azari@equispheres.com (K.A.)
*   Correspondence: mathieu.brochu@mcgill.ca
†   Presented at the 15th International Aluminium Conference, Québec, QC, Canada, 11–13 October 2023.

Abstract: Metal-fused filament fabrication (MF3), which is a variation of the conventional fused filament fabrication (FFF), has recently gained interest due to its distinctive process flexibility and rapid prototyping capability to produce metallic parts. With respect to the additive manufacturing (AM) of aluminum alloys, most efforts have been centered on laser powder bed fusion technologies, with limited activities focused on binder-based processes due to challenges in the sintering of aluminum powders. With respect to MF3, one challenge for fabricating metallic components is the appropriate selection of a binder mixture, enabling the extrusion of a filament with high metallic volume content. In this paper, a mixture of biodegradable aliphatic polyester thermoplastic is used as a binder phase to act as the carrier for AlSi10Mg alloy powders.

Keywords: aluminum alloy; melt blending; printability

1. Introduction

Over the past two decades, additive manufacturing (AM) technologies have advanced to the status of being key digital design tools, where parts are now constructed by adding discrete quantities at a given time. AM has the main advantage of shortening the time from design to final stage [1]. Powder bed fusion (PBF) and direct energy deposition (DED) are, at present, leading AM technologies to produce metallic components [2]. The central differences between these processes lie in the physical form of the feedstock (powder and size, and wire, respectively), as well as energy source (laser and electron beam, respectively).

In contrast to the above-mentioned beam-based approaches, in binder-based processes, including MF3, the raw material is either in the form of a powder or a metal-loaded filament, and it relies on particle bonding through sintering [3].

In MF3 technology, the raw material is fed into a nozzle that heats up to the required temperature and then deposits it layer by layer in a semi-molten state [4]. Researchers have used this technology to successfully print filaments with a high-volume percentage of metal. For instance, in the work of J. Gonzales-Gutierrez et al. [4], MF3 filaments with 55 vol.% of 316L and 17-4PH stainless-steel powders were printed, where the geometry had acceptable GD&T characteristics. In another work, Y. Thompson [5] successfully performed MF3 Inconel 718 parts using a filament containing 55% loading in metal particles.

In this work, a mixture of biodegradable aliphatic polyester thermoplastic was used as the binder phase in a melt blending process, followed by the extrusion of the filament containing 55 vol.% of AlSi10Mg powder to be used in MF3. Microstructural properties and printability are reported.

2. Materials and Methods

The AlSi10Mg powder utilized in this work was provided by Equispheres Inc. (Ottawa, ON, Canada). Poly (lactic acid) (PLA) (Ingeo Bioworks 2003D, MFI = 6 g/10 min (210 °C/2.16 kg), density = 1.24 g/cm^3, D-isomer content = 4.2%) was purchased from Nature-Works LLC (Minnetonka, MN). Tributyl 2-acetylcitrate (ATBC) (98%) was used as a plasticizer and was purchased from Sigma-Aldrich (Oakville, ON, Canada).

The aluminum powder size distribution (PSD) was measured using a Microtrac MRB Sync particle size analyzer. The powder morphology and shape were analyzed using a scanning electron microscope (SEM) (Hitachi SU3500, Tokyo, Japan).

The PLA pellets were dried under vacuum for 24 h at 40 °C to remove residual moisture before usage. Both the metallic powder and plasticizer were used as received. A melt-mixed blend with 55 vol.% in AlSi10Mg powder was fabricated. The blend was prepared using a Rheocord System 40 double-arm internal batch mixer (Haake Buchler, Rheomix, Waltham, MA, USA). The blend was mixed for 10 min at 175 °C at a rotation speed of 40 rpm. Afterward, the batch was cut into small granules prior to extrusion in a single-screw extruder configuration (Haake Buchler). Attached to the screw end was a cylindrical die with a die diameter of 1.80 mm. Filaments with diameter of 1.70 ± 0.05 mm were obtained. To observe this blend under SEM, the VP-SEM mode was operated at a pressure of 60 Pa.

The glass transition (Tg) and melt (Tm) temperatures of the blend were measured via differential scanning calorimetry (DSC) using a TA Instruments Q2000 (New Castle, DE, USA) under a nitrogen atmosphere using the following heat/cool/heat cycle, where the Tg was determined from the reversible heat flow of the second heating cycle using the automated glass/step transition tool in the TA Instruments Universal Analysis 2000 software. The melting (Tm) and cold crystallization (Tcc) temperatures were taken from the second heating scan.

To evaluate the printability of the fabricated filament, cylindrical coupons were printed on an AON M2+ high-temperature industrial 3D printer equipped with an E3D-Volcano (1.75 mm type) hot-end, with a nozzle exit diameter of 0.4 mm. The nozzle temperature, bed temperature, layer height, and infill printing parameters were 190 °C, 30 °C, 0.25 mm, and 100%, respectively.

3. Results and Discussion

The PSD characteristic diameters of the AlSi10Mg powder measured with the PSD analyzer are D10 = 29 μm, D50 = 35 μm, and D90 = 48 μm.

A particular requirement of high-performance feedstock filaments is that the powder particles must be properly distributed and dispersed throughout the filament [5]. Figure 1a depicts the morphology of the virgin AlSi10Mg powder. As shown, the particles are highly spherical. Figure 1b depicts the AlSi10Mg particles embedded in the plasticized–PLA matrix. As shown, the powder particles are well dispersed in the polymeric matrix. An interface between the surface of aluminum particles and the polymeric matrix can be visualized, which could help in the adhesion between printed layers. However, voids within metal particles and the polymer can also be observed.

DSC was used to measure transition temperatures, namely, Tg, Tm, and Tcc temperatures of the blend, in order to tune the extrusion temperatures to be used during MF3. Figure 2 depicts a representative thermogram for a sample, where exothermic and endothermic peaks corresponding to the transition temperatures can be seen. The Tg, Tcc, and Tm are measured to be 49, 105, and 150 °C, respectively. With respect to Tm, a double endothermic peak is shown in the thermogram, which is ascribed to the melting–recrystallization process from a phase that melts at a lower temperature [6].

Printing via MF3 of the blend selected in this work was adjusted for highly filled filaments to mainly consider thermal properties such as Tm and Tg. In this context, Tg was above room temperature; so, to help the adhesion to the printing surface, a bed temperature of 40 °C, which is near the Tg of the blend, was also applied, in addition to the printing

parameters mentioned in the previous section. Hence, as the Tm of the used filament is around 150 °C, it is recommended [4–6] that a nozzle temperature above the melting point of the binder be used in order to improve adhesion between layers and ensure stability.
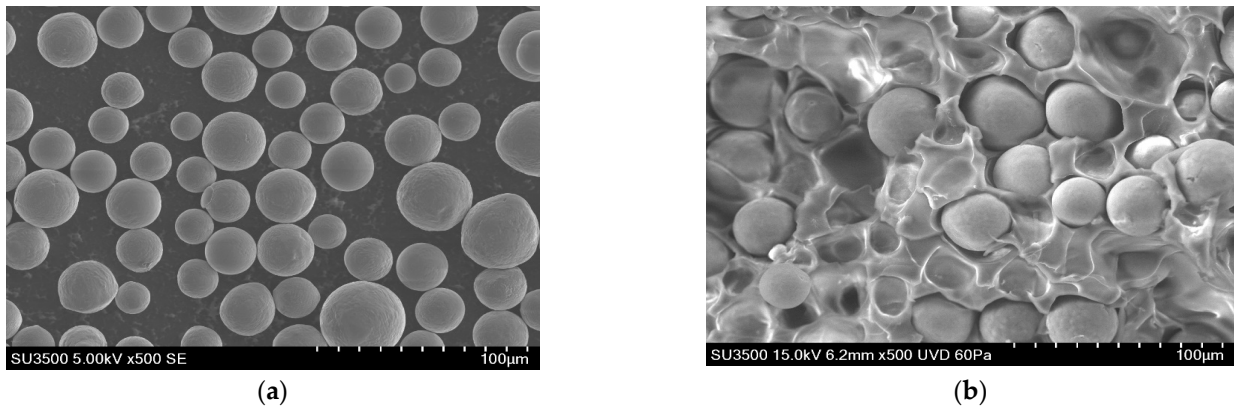

(**a**)

(**b**)

Figure 1. SEM micrographs of (**a**) AlSi10Mg virgin powder and (**b**) PLA matrix with embedded AlSi10Mg particles.
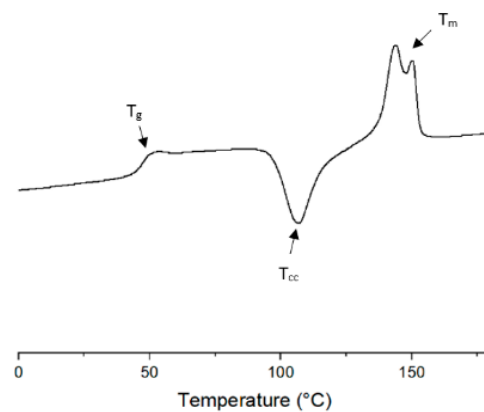
Figure 2. DSC thermogram of the PLA/AlSi10Mg powder blend.

As seen in Figure 3, using the above-mentioned printing parameters, it was possible to extrude and produce the highly loaded filament, which when printed achieved good adhesion between layers in the printed part. Hence, this result could help to attain high densities after debinding and sintering. However, parameters have to still be adjusted to avoid void formation as much as possible, which we are now actively determining.
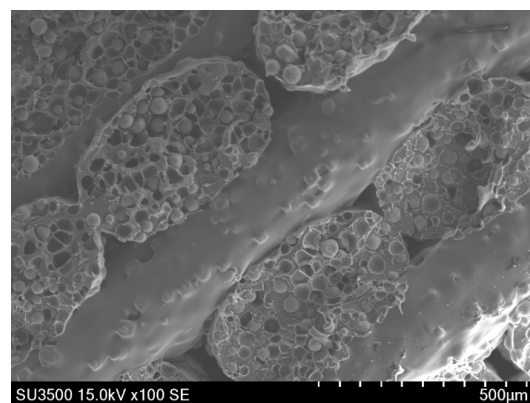

Figure 3. SEM micrograph of the 3D printed part using PLA/AlSi10Mg powder filament.

4. Conclusions

Highly loaded filaments with 55% AlSi10Mg powder were successfully MF3 using an industrial 3D printer, with DSC analysis being used as the main tool to set the main printing parameters. Also, a good degree of dispersion was achieved upon melt mixing of the powder with the binder, which will help in further processing steps, including debinding and sintering.

References

1. Thompson, Y.; Gonzalez-Gutierrez, J.; Kukla, C.; Felfer, P. Fused filament fabrication, debinding and sintering as a low cost additive manufacturing method of 316L stainless steel. *Addit. Manuf.* **2019**, *30*, 100861. [CrossRef]
2. Atatreh, S.; Alyammahi, M.S.; Vasilyan, H.; Alkindi, T.; Susantyoko, R.A. Evaluation of the infill design on the tensile properties of metal parts produced by fused filament fabrication. *Results Eng.* **2023**, *17*, 100954. [CrossRef]
3. Wagner, M.A.; Hadian, A.; Sebastian, T.; Clemens, F.; Schweizer, T.; Rodriguez-Arbaizar, M.; Carreño-Morelli, E.; Spolenak, R. Fused filament fabrication of stainless steel structures—From binder development to sintered properties. *Addit. Manuf.* **2022**, *49*, 102472. [CrossRef]
4. Chohan, J.S.; Singh, R. Pre and post processing techniques to improve surface characteristics of FDM parts: A state of art review and future applications. *Rapid Prototyp. J.* **2017**, *23*, 495–513. [CrossRef]
5. Thompson, Y.; Zissel, K.; Förner, A.; Gonzalez-Gutierrez, J.; Kukla, C.; Neumeier, S.; Felfer, P. Metal fused filament fabrication of the nickel-base superalloy IN 718. *J. Mater. Sci.* **2022**, *57*, 9541–9555. [CrossRef] [PubMed]
6. Zhu, D.; Ren, Y.; Liao, G.; Jiang, S.; Liu, F.; Guo, J.; Xu, G. Thermal and mechanical properties of polyamide 12/graphene nanoplatelets nanocomposites and parts fabricated by fused deposition modeling. *J. Appl. Polym. Sci.* **2017**, *134*, 45332. [CrossRef]